Dendrites Regularized by Spatially Homogeneous Time-Periodic Forcing

T. Börzsönyi, T. Tóth-Katona, Á. Buka, and L. Gránásy

Research Institute for Solid State Physics and Optics, Hungarian Academy of Sciences, P.O.B. 49, H-1525 Budapest, Hungary

(Received 13 April 1999)

The effect of spatially homogeneous time-periodic external forcing on dendritic solidification has been studied by phase-field modeling and experiments on liquid crystal. It is shown that the frequency of dendritic sidebranching can be tuned by oscillating pressure or heating. The main parameters that influence this phenomenon are identified.

PACS numbers: 81.10.Aj, 64.70.Dv, 64.70.Md, 68.70.+w

One of the most spectacular and practically important growth modes observed in nature is dendritic solidification [1]. A dominant part of the present knowledge on dendrites originates from studies on transparent organic model systems [1,2]. The nonlinearity of the problem implies that periodic external perturbations may lead to specific resonance patterns that could be used for regulating the growth morphology. The understanding of dynamic response to such perturbations could open a novel route to materials of application tailored properties.

A spatially inhomogeneous controlling of dendritic sidebranching has already been achieved by periodic local heating of the dendrite tip by laser beam [3], or by oscillatory flow field [4]. In this work we explore the possibility of controlling dendritic growth homogeneously throughout the sample via pressure oscillations that influence the melting point, and uniform periodic heating in the volume. We use the phase-field model, an approach that is able to handle all stages of morphology evolution including dendritic growth [1,5,6], to identify the most important process parameters and resonance conditions in two dimensions (2D). The predictions are tested by experiments on quasi-2D liquid crystal layers, known as suitable model materials [7].

The phase-field model represents a dynamic extension of the Cahn-Hilliard theory of first-order phase transformations that couples the evolution of the order-parameter distribution [$\phi(\mathbf{r},t)$ = phase field] to thermal transport [1,5,6]. The respective equations that incorporate the anisotropy of both the interfacial free energy [$\sigma(\theta) = \sigma_o\tilde{\sigma}(\theta)$] and kinetic coefficient [$\beta(\theta) = \beta_o\tilde{\beta}(\theta)$] read as follows [8]:

$$\epsilon^2\tau_o\tilde{\beta}\tilde{\sigma}\frac{\partial\phi}{\partial t} = \phi(1-\phi)\left\{\phi - \frac{1}{2} + 30\epsilon\alpha\Delta[u - A(t)]\phi(1-\phi)\right\} - \epsilon^2\frac{\partial}{\partial x}\left[\tilde{\sigma}\tilde{\sigma}'\frac{\partial\phi}{\partial y}\right] + \epsilon^2\frac{\partial}{\partial y}\left[\tilde{\sigma}\tilde{\sigma}'\frac{\partial\phi}{\partial x}\right] + \epsilon^2\nabla[\tilde{\sigma}^2\nabla\phi], \quad (1)$$

$$\frac{\partial u}{\partial t} + \frac{1}{\Delta}30\phi^2(1-\phi)^2\frac{\partial\phi}{\partial t} = \nabla^2 u + B(t), \quad (2)$$

where $u(\mathbf{r},t) = (T - T_r)/(T_r - T_\infty)$ is the dimensionless temperature, $\tilde{\sigma}' = d\tilde{\sigma}/d\theta$, and the relevant physical properties are combined to form dimensionless parameters $\Delta = c_p(T_r - T_\infty)/L$, $\alpha = \sqrt{2}\,\omega S_m L/(12 c_p\sigma_o)$, $\tau_o = S_m D\beta_o/\sigma_o$, and $\epsilon = \delta/\omega$, with S_m, L, T_m, c_p, D, and δ standing for the melting entropy, enthalpy, and temperature, the specific heat, the thermal diffusion coefficient, and the interface thickness. Lengths and time are scaled by a reference length ω (comparable to the size of the well developed germ) and ω^2/D, respectively. Other details of the numerical method are given in Ref. [7(b)]. Contrary to the usual definition of the dimensionless temperature in terms of the melting point, u is related here to a reference temperature T_r. This is needed to avoid difficulties when introducing an oscillatory melting point. The problem is invariant to the choice of T_r, provided that $A = u_m = (T_m - T_r)/(T_r - T_\infty)$ is inserted into Eq. (1). (With $T_r = T_m$ the usual form of the phase-field model is recovered.)

The external perturbations appear in the governing equations as follows.

(A) Pressure modulations [$A(t) = u_m(t) = a_0 f(t)$ and $B(t) = 0$].—The dominant effect is the variation of the melting point (and thus the undercooling) with pressure according to the Clausius-Clapeyron relationship $T_m = T_m(p_0) + (p - p_0)\Delta V/S_m$, where ΔV is the volume change upon solidification. This effect receives considerable attention currently [9] owing to its capacity to change the undercooling instantaneously and uniformly in large volumes [10].

(B) Periodic heating in the volume [$A(t) = 0$ and $B(t) = b_0 f(t)$].—It is represented by the source term $B(t)$ in the heat transport equation Eq. (2).

The phase-field equations have been solved numerically on a rectangular $N \times N$ lattice ($N = 1000$) for the free growth of a crystallite just nucleated at the center $(x, y = 0)$ of a square liquid region (see Fig. 1). For

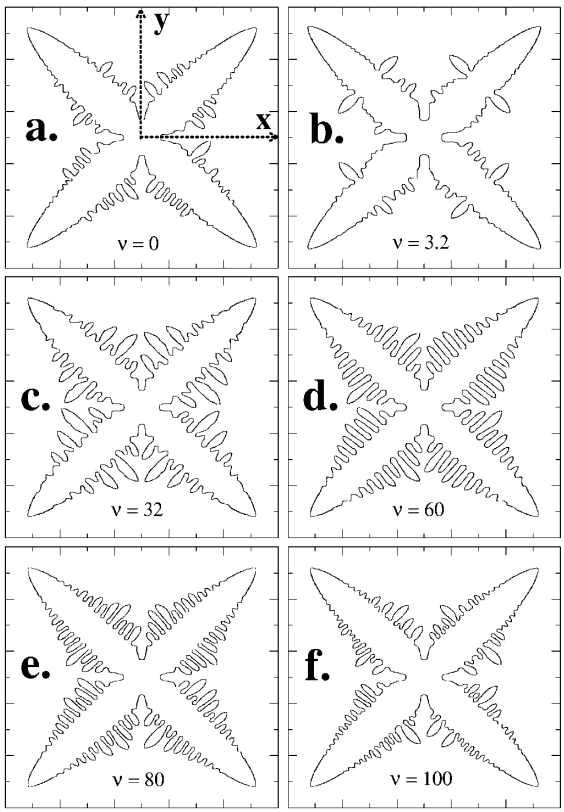

FIG. 1. (a)–(f): The effect of square-wave pressure perturbation on the solidification morphology. $a_0 = 0.2$ and $\xi = 0.3$; $\nu = 0$ (no pressure oscillation), 3.2, 32, 60, 80, and 100, respectively; $t = 0.24$; $\Delta = 0.55$; $\sigma_4 = 0.12$; $\beta_4 = 0.24$; $\alpha = 350$; $\tau_0 = 20$; $\varepsilon = 0.005$; system size: 1000×1000 pixels (that corresponds to 5×5 in dimensionless units); time-step: 0.0001 [13].

the comparison with the experimental system a fourfold symmetry has been assumed for the angular dependencies $\tilde{\sigma} = 1 + \sigma_4 \cos(4\theta)/2$ and $\tilde{\beta} = 1 + \beta_4 \cos(4\theta)/2$, where σ_4 and β_4 are the anisotropy parameters. In each time step a spatially uncorrelated noise with the amplitude of 0.01 was added to u. The regularity of the growth patterns is characterized by the quantities a and b:

$$a = \frac{\sum_{i,j=-N/2}^{N/2} (\phi_{i,j} - \phi_{-i,j})^2}{M}, \tag{3}$$

$$b = \frac{\sum_{i,j=-N/2}^{0} (\phi_{i,j} - \phi_{j,i})^2}{K}, \tag{4}$$

where M and K are the numbers of pixels in which $0.4 < \phi < 0.6$ for the whole system and for the lower left quarter, respectively. As for a the summation runs for all pixels, $a \geq 0$ measures the axisymmetry of the whole domain relative to the y axis, while $b \geq 0$ measures the axisymmetry of one main branch. Both parameters are zero for symmetric patterns.

To identify the range of conditions under which periodic external perturbations dominate the pattern formation, we investigated the parameter space defined by the amplitude and the frequency of the modulation, the undercooling, and the anisotropy.

First, we address the consequences of pressure oscillations that translate into an oscillatory melting point via the Clausius-Clapeyron law. Sinusoidal, $f(t) = [\sin(2\pi\nu t) + 1]/2$, and square-wave (with filling coefficient $\xi = t_{\text{on}}/t_0$, where t_0 is the period of oscillations and t_{on} stands for the pulse length) modulations were studied.

The response to a square-wave modulation with $a_0 = 0.2$ and $\xi = 0.3$ is presented in Fig. 1 as a function of the dimensionless modulation frequency ν. Using $\sigma_4 = 0.12$, $\beta_4 = 0.24$, and $\Delta = 0.55$ (the latter follows from the known limitations of phase-field modeling [1,11]), the unmodulated state displays irregular sidebranching due to the effect of the noise [Fig. 1(a)]. At low frequencies (where the switching transient is negligible), the pressure modulation leads to alternating steady-state growth regimes corresponding to a lower and a higher undercooling, the latter characterized by enhanced sidebranching [Fig. 1(b)].

A regular morphology is observed in the dimensionless frequency range $15 < \nu < 90$, which is slightly below the frequencies of the noise induced (early stage) sidebranches of the dendrites ($\nu = 70$–210 at the location of 10–1 tip radii behind the tip) emerging from the microscopic solvability theory [12]. In this regime, the formation of sidebranches [Figs. 1(c)–1(e)] and the tip velocity (Fig. 2) show a strict correlation with pressure (undercooling) pulses. The increasing regularity of growth patterns is manifested in a minimum of the symmetry parameters around $\nu \sim 30$ (Fig. 3). As the frequency increases further, the front is unable to follow the external perturbation, and the uncorrelated weak thermal sidebranching reappears [Fig. 1(f)]. Similar results have been obtained for sinusoidal oscillations.

Increasing the undercooling the tendency for spontaneous sidebranching becomes more pronounced; the external perturbations need only to regulate them. At small undercoolings, however, the large anisotropy hinders spontaneous sidebranching, and external perturbations are needed to trigger them, reflected in less developed sidebranches.

The calculations performed at various degrees of anisotropy show that regular morphology may form only if the anisotropy is high enough. Without well defined orientational preferences the external perturbations are unable to drive the amoebaelike growth forms into a regular pattern.

Computations for alternating *heating and cooling* lead to essentially the same type of resonance patterns as pressure oscillations, provided that the average heat production for a period was negligible. However, in the case of oscillatory *heating*, the introduction of a local off-plane thermal transport was necessary to prevent the melting of the crystallite for heating amplitudes needed to generate regular patterns. The off-plane heat transport has been taken

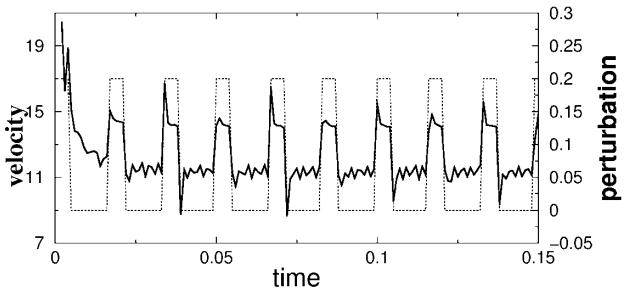

FIG. 2. The tip's velocity in time (solid line) and the melting point $u_m = A(t)$ (dotted line) for $\nu = 60$ [Fig. 1(d)] in dimensionless units.

into account via a dimensionless heat transfer coefficient h leading to $B(t) = b_0 f(t) + h[u(\mathbf{r}, t) - u_\infty]$.

These investigations imply that under well defined conditions both types of oscillatory perturbations can be used to control dendritic solidification.

To test the predictions, experiments have been performed on thin liquid crystal layers. The nematic-smectic $B(N - S_B)$ phase transition of liquid crystals is recognized as an appropriate model of crystallization in liquids with high anisotropy of $\sigma(\theta)$ [7]. Ready-made cells of E. H. C. Co. (Japan) KSRP-10 (of thickness 10 μm) and KSRP-02 (2 μm) have been filled with CCH3 (Merck, Darmstadt). The surface treatment of the bounding glass plates assured the planar alignment of both N and S_B phases [the directors $\mathbf{n}(N)$ and $\mathbf{n}(S_B)$ are in the plane of the cell] and the conducting layers on the bounding plates were used as electrodes.

For pressure modulation the liquid crystal cell was placed into a brass box surrounded by a temperature controlled hot stage of accuracy ± 3 mK. The gas pressure in the brass box has been regulated by a computer controlled valve system that switches on and off an excess pressure p_e preset between 0 to 2 bars with an accuracy of ± 0.03 bar. We measured the pressure coefficient of the phase transition temperature and found it about 0.035 K/bar.

The modulated heat release in the bulk has been realized by periodically transmitting a high frequency (600 kHz) electric current through the LC layer, which leads to a heat evolution in the bulk. The local off-plane heat transport

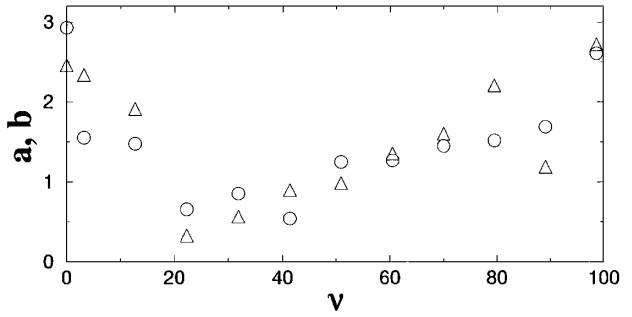

FIG. 3. The frequency dependence of the symmetry parameters a (○) and b (△). (Other parameters are as for Fig. 1.)

(the precondition of regulation with oscillatory heating) is ensured by sample geometry through the bounding plates.

Square-wave oscillations of both pressure and heating power have been applied in the experiments. The best correlation between sidebranching and external perturbations has been observed for large modulation amplitudes (2 bars or 3×10^{-4} W/cm^2). These amplitudes have comparable effects on undercooling ($\sim$0.1 K), as estimated on the basis of the pressure coefficient of the melting point and other relevant properties.

In accord with the simulations, there is an upper limit for the period-averaged heating power ($\overline{P} \sim 10^{-4}$ W/cm^2) above which even the off-plane thermal transport does not prevent the melting of the dendrites. The most regular resonance patterns were observed for short pressure (or current) pulses in the range of $\xi = 0.1$–0.3.

The experimental results are summarized in Fig. 4. Without perturbation, the sidebranching is essentially random [Figs. 4(a) and 4(d)]. Under oscillatory pressure or electric field "resonance patterns" of fairly regular sidebranches appear [see Figs. 4(b), 4(c), 4(e), and 4(f)]. As predicted by the phase-field calculations, the sidebranch formation correlates with the external perturbations in a wide frequency range. This correlation is demonstrated in Fig. 4(f), where the black lines denote the position of the

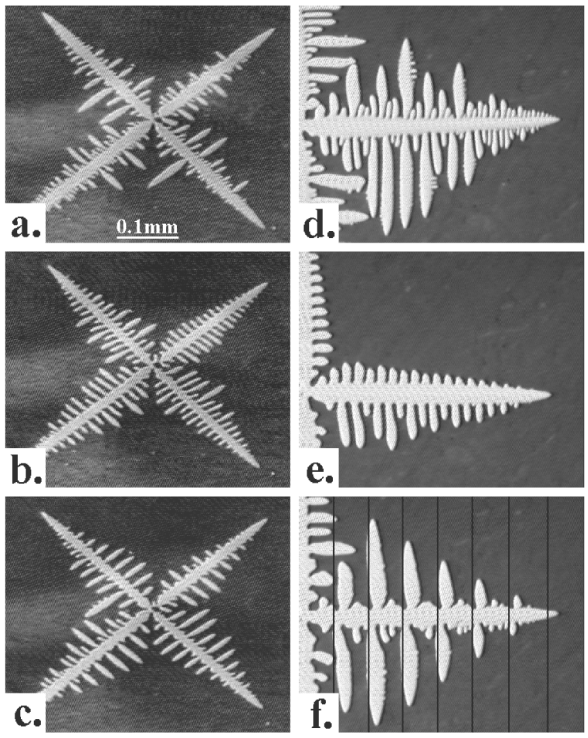

FIG. 4. Effect of the oscillatory pressure [(a)–(c)] and electric current [(d)–(f)] on the smectic-B dendrite growing in undercooled nematic phase ($\Delta T = 1.0$ °C). (a) No oscillations; (b) $t_0 = 0.61$ s, $\xi = 0.2$, $p_e = 2$ bars; (c) $t_0 = 1.1$ s, $\xi = 0.2$, $p_e = 2$ bars; (d) no oscillations; (e) $t_0 = 2.15$ s, $\xi = 0.16$, $\overline{P} = 6 \times 10^{-5}$ W/cm^2; (f) $t_0 = 5.12$ s, $\xi = 0.14$, $\overline{P} = 6 \times 10^{-5}$ W/cm^2.

tip at the centers of the heating pulses. A remarkable feature is the shift in the position of the sidebranches on the two sides of the main tip. This might be attributed to the asymmetry of the dendrite tip. In line with our theoretical predictions (Fig. 2), oscillations have been detected in the tip velocity, however, of an amplitude that is just above the resolution of the present experimental setup.

Finally, one should note that the electric heating in liquid crystals may have side effects that are not incorporated into our phase-field model. For example, switching on the electric field the nematic director $\mathbf{n}(N)$ changes from planar to homeotropic (perpendicular to the bounding plate) that affects σ and its anisotropy, and induces a local flow in the sample. For this class of materials these phenomena should also be included in a quantitative description of the problem.

To summarize, our computer simulations and experiments demonstrated that dendritic sidebranching can be regulated by spatially homogenous (nonlocalized) periodic variation of the melting point (induced by oscillatory external pressure) or by periodic heating (generated by a dissipative electric current). Both effects influence the growth velocity of the moving dendritic tip, and lead to the formation of a regular set of sidearms, a phenomenon that diminishes with decreasing interfacial/kinetic anisotropy. A detailed understanding of the dynamic response of crystallizing systems to such perturbations might open new routes in designing materials.

This work was supported by research Grants No. OTKA T014957, No. T025139, and No. F022771. The computations were performed on computers donated by the Alexander von Humboldt Foundation.

[1] *Handbook of Crystal Growth,* edited by D. T. J. Hurle (North-Holland, Amsterdam, 1993), Vol. 1B.

[2] S. C. Huang and M. E. Glicksman, Acta Metall. **29**, 701 (1981); M. E. Glicksman and N. B. Singh, J. Cryst. Growth **98**, 277 (1989); E. R. Rubinstein and M. E. Glicksman, J. Cryst. Growth **112**, 84 (1991); **112**, 97 (1991); M. E. Glicksman and S. P. Marsh, in Ref. [1], p. 1077.

[3] X. Qian and H. Z. Cummins, Phys. Rev. Lett. **64**, 3038 (1990); L. Williams, M. Muschol, X. Qian, W. Losert, and H. Z. Cummins, Phys. Rev. E **48**, 489 (1993); B. T. Murray, A. A. Wheeler, and M. E. Glicksman, J. Cryst. Growth **154**, 386 (1995).

[4] Ph. Bouissou, A. Chiffaudel, B. Perrin, and P. Tabeling, Europhys. Lett. **13**, 89 (1990).

[5] A. Karma and W. J. Rappel, Phys. Rev. Lett. **77**, 4050 (1996); Phys. Rev. E **57**, 4323 (1998).

[6] O. Penrose and P. C. Fife, Physica (Amsterdam) **43D**, 44 (1990); S.-L. Wang, R. F. Sekerka, A. A. Wheeler, B. T. Murray, S. R. Coriell, R. J. Braun, and G. B. McFadden, Physica (Amsterdam) **69D**, 189 (1993).

[7] (a) Á. Buka, T. Tóth-Katona, and L. Kramer, Phys. Rev. E **51**, 571 (1995); T. Tóth-Katona, T. Börzsönyi, Z. Váradi, J. Szabon, Á. Buka, R. González-Cinca, L. Ramirez-Piscina, J. Casademunt, and A. Hernández-Machado, Phys. Rev. E **54**, 1574 (1996); (b) T. Börzsönyi, Á. Buka, and L. Kramer, Phys. Rev. E **58**, 6236 (1998).

[8] G. B. McFadden, A. A. Wheeler, R. J. Braun, and S. R. Coriell, Phys. Rev. E **48**, 2016 (1993).

[9] J. C. La Combe, M. B. Koss, L. A. Tennenhouse, E. A. Winsa, and M. E. Glicksman, J. Cryst. Growth **194**, 143 (1998); M. B. Koss *et al.*, Transient Dendritic Solidification Experiment, Proposal No. 96-HEDS-02-216, submitted in response to NASA Research Announcement, Microgravity Materials Science: Research and Flight Experiment Opportunities, NRA-96-HEDS-02.

[10] The regulation of dendritic growth via pressure changes has been proposed by G. Szabó (Research Institute of Materials Science, Budapest) as early as 1982.

[11] Y.-T. Kim, N. Provatas, N. Goldenfeld, and J. Dantzig, Phys. Rev. E **59**, R2546 (1999).

[12] J. S. Langer, Phys. Rev. A **36**, 3350 (1987); M. Ben Amar and Y. Pomeau, Europhys. Lett. **2**, 307 (1986); D. C. Hong and J. S. Langer, Phys. Rev. A **36**, 2325 (1987).

[13] Computer animations based on our simulations are displayed at http://www.kfki.hu/~btamas/phase/perturb.html